Permanent Magnet Linear Motors for Short Strokes

Bruno Lequesne, *Senior Member, IEEE*

Abstract—**The use of new powerful permanent magnet materials such as Neodymium-Iron-Boron alloys can greatly improve the performance of electrical machines. The paper analyzes the impact of their use on linear motors with particular emphasis on fast action over strokes on the order of 5 to 20 mm. Closed-form formulae, which link the travel time to the stroke and heat dissipation limit of the device, are established. These formulae are used to compare various machine configurations, some of which were devised specifically for this application. It is shown that permanent magnet linear motors feature very fast travel times, but can do so only at low duty cycles. For that reason, two-spring actuators [1] though not as fast for single motion are superior when higher frequencies of operation are required.**

I. Introduction

PERMANENT magnet machines have been used for linear motion for some time, as in "voice-coil motors" for speakers. In these motors, stationary magnets exert a force on a moving coil, usually built without an iron core for lower inertia. These machines have also been used in positioning applications, particularly in the computer industry, because of the linearity of their force-current relationship as well as their low inertia [2]–[4]. The fragility of the moving coil connection has limited, however, both the possible range of motion and the harshness of the environment in which they could be used.

The introduction of the more powerful Neodymium-Iron-Boron magnets has enabled the improvement of the performance of voice-coil motors as it allowed, in a similar fashion, the improvement of brushless permanent magnet motor drives. In particular, it makes it conceivable to construct the motor with moving magnets, rather than a moving coil, without paying an insurmountable penalty in terms of inertia [5]. The result would be a more rugged and less expensive construction capable of longer strokes and of applications in harsher environments, including, possibly, automotive [6]–[8].

These new avenues have already received some theoretical attention. For example, Honds and Meyer designed a motor with a constant force over a 250-mm stroke, and provide force formulae based on reluctance calculations [9]. Smith and Appel perform a finite-element calculation of thrust in a machine with a 12-mm stroke [10], and address analytically the important question of side loading, particularly in misaligned devices [11]. Basak and Shirkoohi also use finite elements for this problem [12]. Pelissier *et al.*, show briefly how an optimization routine can be applied to these devices [13]. These papers, however, analyze specific designs. In the present paper, only a design goal is specified, namely fast actuation over a stroke on the order of 5 to 20 mm, and an attempt is made to evaluate and compare various viable configurations.

To that end, an original closed-form solution was devised. The finite element method, used exclusively in [10] and [12], is used here also for convenience and accuracy to calculate such machine parameters as force and inductance. These parameters are then used as part of a formula for the displacement time versus position which incorporates the heat-dissipation limit of the device.

This analysis allows the selection of the best configuration, and then the comparison of its potential performance with competing schemes, such as solenoids with moving magnets [14], which rely on repulsion forces on the magnets to provide a strong initial acceleration, or with 2-spring solenoids [1] which rely on compressed springs for initial thrust. Linear motors based on variable-reluctance principles are also possible [15]–[17], but were not considered in this study. They were compared in [17] with permanent magnet devices.

Paper IPCSD 95–56, approved by the Electric Machines Committee of the IEEE Industry Applications Society for presentation at the 1992 Industry Applications Society Annual Meeting, Houston, TX, October 4–9. Manuscript released for publication August 10, 1995.

The author is with the Electrical and Electronics Department, General Motors Research and Development Center, Warren, MI 48090-9055 USA.

Publisher Item Identifier S 0093-9994(96)00308-8.

II. Device Description and Analysis

A. General Configuration

Fig. 1 shows a possible configuration with a stationary magnet and a moving coil wound around the axis. Cylindrical geometries were assumed in this study.

Two types of forces act on the moving armature. On one hand, when a dc voltage is switched across the coil, it gives rise to a current i which interacts with the magnet's field B to create a force F_c, according to Lenz's law

$$F_c = i\vec{X}_c \times \vec{B} \tag{1}$$

where X_c is the length of the conductor exposed to the magnetic field. The flux density provided by the magnet is determined primarily by the magnet material and its reluctance path. It changes little as the armature moves. The demagnetization effect due to the coil current is small, because the flux created by the current is perpendicular to that of the magnet. Therefore, B is approximately constant and F_c is proportional to the current [10].

Another force, F_s, is exerted by the leakage flux on the extremities of the armature. This force may be desirable to latch the armature at both ends of travel, and can be increased if necessary by including pole extensions on the stator, as shown in Fig. 1. This force F_s drops rapidly as motion starts. In general, it must be designed to be no larger than necessary for latching purposes, in order to minimize energy requirements.

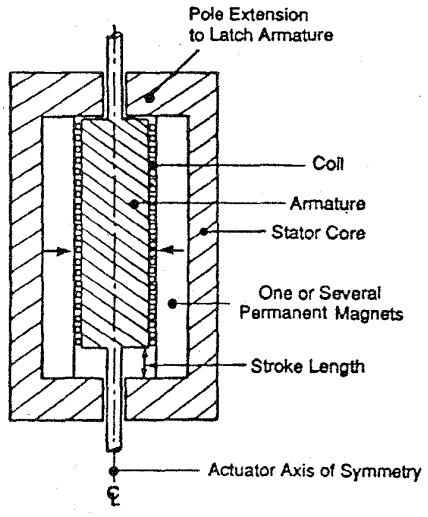

Fig. 1. General configuration.

Theoretical developments, such as force calculations, etc., are the same regardless of whether the magnets are stationary or moving. The differences between the stationary-and moving-magnet configurations are of a practical nature: Moving coils mean lower inertia, except, possibly, with modern powerful magnets, but require special arrangements to connect the currents to the moving part. Brushes must be used, or, in this case and because of the short stroke, flexible wires. Stationary coils may require a position sensor.

B. Flux-Density and Magnetic-Force Calculation

The analysis of these linear actuators requires first the solution of the magnetic field problem. Since the devices are cylindrical, they are axisymmetric and the problem can be solved in a two-dimensional plane. An analytical solution based on reluctance calculations is possible. Since such a solution was developed in [9], it is not repeated here and a finite-element program [18] is used instead, for convenience and accuracy. An algorithm based on Maxwell's stress tensor is then used to calculate the total magnetic force, F

$$F = F_c + F_s. \tag{2}$$

With the proper definition of the integrating surfaces, the terms F_c and F_s can be calculated separately [19]. Since F_c is proportional to current and relatively independent of position, it needs to be calculated only in one position and can be characterized by the acceleration-per-Ampere-turns ratio λ_c (in m/s^2/At), after division by the moving mass m

$$\lambda_c = \frac{F_c}{mNi} = \frac{F - F_s}{mNi} \tag{3}$$

where N is the number of turns. If F_s relatively small (up to 15%), one may use instead the ratio λ (in m/s^2/At), defined as

$$\lambda = \frac{F}{mNi}. \tag{4}$$

The finite element method can also be used to calculate the flux linkages for various current levels, from which the total inductance can be deduced. Finally, it allows to check the saturation levels in the core and the flux-density level in the permanent magnet. The latter is of particular importance for high temperature applications, to check that the flux density does not drop below demagnetization level.

C. Travel Time: Closed-Form Solution

The coils are excited by switching a constant voltage V across the coils. The current flow is governed by the electric circuit equation

$$V = iR + N\frac{\partial \phi}{\partial i}\frac{di}{dt} + N\frac{\partial \phi}{\partial x}\frac{dx}{dt} \tag{5}$$

where R is the coil resistance and ϕ is the flux linkage in the coils.

At the beginning of motion, the velocity is small and the back-emf term, i.e., the last term in (5), is negligible. Also, since a fast current rise and minimal copper losses are of primary importance, the coils must have a low resistance. Therefore, at the beginning of motion and as a first degree approximation, (5) can be written

$$V = N\frac{\partial \phi}{\partial i}\frac{di}{dt} = L\frac{di}{dt} \tag{6}$$

where L is the inductance. The above formula remains valid until the velocity becomes significant. In actuators with a relatively short stroke as in the case here, this happens only shortly before the end of the stroke, therefore the back-emf can be neglected altogether.

Then, integrating (6) yields

$$Ni = (V'/L')t \tag{7}$$

where $V' = V/N$ and $L' = L/N^2$.

Neglecting friction and taking into consideration (4), the equation of motion is

$$m\ddot{x} = F = m\lambda Ni. \tag{8}$$

Replacing (Ni) in (8) by its expression in (7) and integrating, the displacement is

$$x = \lambda\frac{V'}{L'}\frac{t^3}{6}. \tag{9}$$

Solving (9) yields the travel time $t = t_m$ that corresponds to $X = X_1$ where X_1 is the total stroke, thereby characterizing the actuator's performance with a closed-form solution. As was noted earlier, this result is obtained by neglecting the back-emf. Because the back-emf tends to reduce the current, the result is optimistic. The validity of the approximation can ultimately be checked by computing the back-emf voltage drop and comparing it to the source voltage, as shown in the Appendix.

For a given stroke X_1 there are therefore two key design parameters, the inductance L' and the ratio λ. As seen in (9), the travel time t_m is smallest when the ratio (L'/λ) is smallest.

D. Limitation in Heat Dissipation

The developments leading to (9) assume that the voltage V remains on throughout the motion. This may not always be possible because of thermal considerations. A more general relationship between travel time t_m, stroke X_1 and maximum allowable current density is provided in the Appendix.

E. Limitation in Device Length

One may think that longer actuators move faster, however, it can be shown in general that at some point, lengthening the armature has no effect on the speed of operation. Consider the equation of motion

$$F = m\ddot{x} = (m_a + m_v)\ddot{x} \tag{10}$$

where the total mass m is the sum of the armature mass, m_a, and the mass of the apparatus to the moved by the actuator, m_v. The magnetic force F is also proportional to the conductor length, see (1), therefore it is proportional to the armature mass with a coefficient $k = F/m_a$. Therefore

$$\ddot{x} = \frac{km_a}{m_a + m_v}. \tag{11}$$

If the device is sufficiently long that $m_a \gg m_v$, then $\ddot{x} \cong k$. The travel time is then independent of armature mass and length.

III. Design Choice

Several possible configurations are now analyzed. The overall dimensions, a length of 110 mm and a diameter of 89 mm, were selected to allow a meaningful comparison with the 2-spring actuators analyzed in [1]. Also, with an armature mass of at least 60% of the total moving mass, the length is at or near the limit beyond which no improvement in speed of operation can be expected.

A. Optimum Number of Poles

Fig. 1 shows a single-pole configuration with one magnet polarity throughout the length of the device, and one coil mounted on a steel armature. Its main advantage is the simple, one-coil design. A moving coil is shown, but again from the point-of-view of magnetic force production, any conclusion applies equally well to moving-coil or moving-magnet configurations.

The most salient feature of this configuration is a prohibitively large latching force, calculated to be -877 N with 6000 At for this case. It is inherent to this design since the magnet flux has no other path but through the top and bottom parts of the moving armature. In addition, the armature core is heavily saturated (ca. 2.8 T), resulting in a low flux density in the permanent magnet (ca. 0.3 T) which makes it vulnerable to demagnetization at higher temperature. The single-pole configuration is therefore unacceptable.

A configuration with four poles is shown in Fig. 2. As the number of poles is increased, saturation diminishes in the armature core and reluctance decreases, resulting in higher air gap flux densities and higher forces. This advantage, though, is offset by the need to match the current flow direction with the various magnet polarities. Electronic commutation with a position sensor, or brushes, could be used. However, if the stroke is small, there is an opportunity for a special, more simple design. Namely, the coils can be concentrated in specific areas of the armature to avoid overlap. While this results in nonoptimum space utilization, it has the deciding advantage of simplicity and is adopted here.

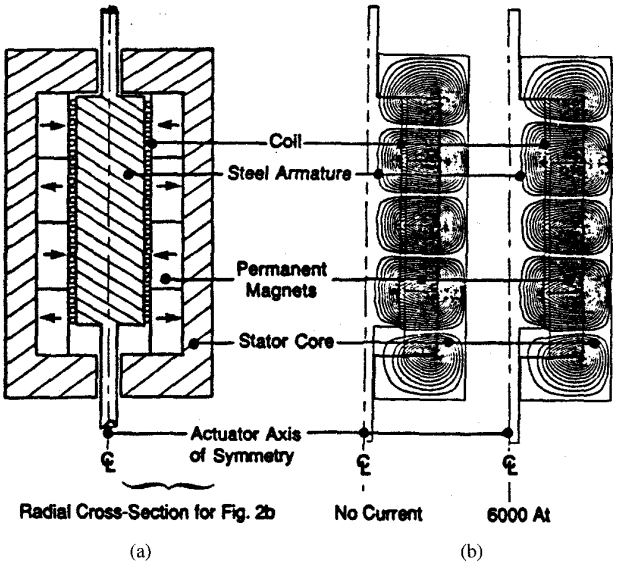

Fig. 2. Multipole configuration. (a) Device layout. (b) Flux plots.

It is shown now that, with such a concentrated-coil design, there is an optimum number of poles for a specific application. A space as long as the stroke X_1 must be left unoccupied between the coils. Denoting X_a the total armature length, the useful armature length X_u for a p-pole configuration is

$$X_u = X_a\left(1 - \frac{(p-1)X_1}{X_a}\right). \tag{12}$$

This decrease in useful armature length is linear with the number of poles and, at some point, it offsets the force improvement resulting from increased air gap-flux densities. This point corresponds to the optimum number of poles.

Calculations were conducted for configurations with 2 and 4 poles and with the coils assumed mounted on a steel armature. The results are presented in Table I. Based on the ratio λ_c, the 4-pole design is preferable to the 2-pole one by a factor of almost 2 to 1. No calculation was conducted either in the 5-pole or the 3-pole cases but no significant increase in force/At is expected. This is because the 4-pole configuration features a high air gap flux density (80% of the magnet's remanent flux density), despite of a high maximum flux density in the core (2.1 T).

B. Armature Design: Magnetic Versus Nonmagnetic Core

The previous section analyzed the case of a coil wound on a steel core. An alternative, using a light-weight, nonmagnetic core material is shown in Fig. 3. The expected performance is summarized in Table II.

TABLE I
INFLUENCE OF THE NUMBER OF POLES ON PERFORMANCE

Number of Poles	Latching Force (N)	Force with 6000 At (N)	λ ($m/s^2/At$)	λ_c ($m/s^2/At$)	Saturation Level, Maximum (T)	Magnet Magnetization, Minimum (T)
2	-883	-425	0.194	0.113	3.0	0.6
4	-394	+368	0.322	0.206	2.1	0.7

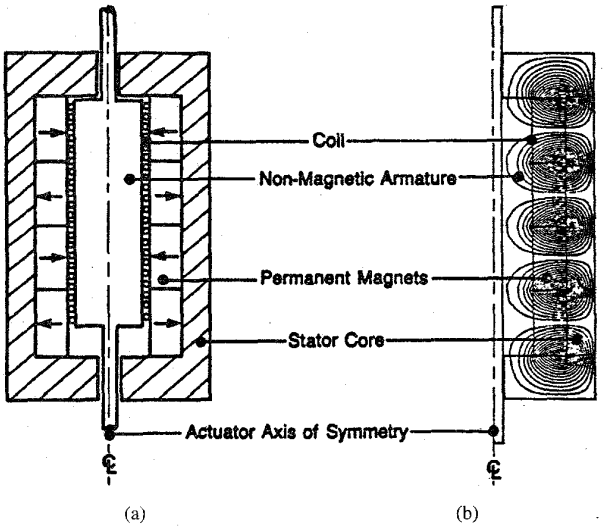

Fig. 3. Configuration with nonmagnetic armature. (a) Device layout. (b) Flux plot, no current.

A nonmagnetic armature has the advantage of a smaller moving mass (130 g versus 394 g in this case) but also the disadvantage of lower flux densities, thus less force. As seen in Table II, the 4-pole configuration is again better than the 2-pole design. Also, λ_c is higher by 42% with a nonmagnetic core, showing that the reduction in moving mass can offset the decrease in magnetic force.

The choice of the armature design, however, must also take other criteria than acceleration into consideration. In particular, a nonmagnetic armature makes it more difficult to dissipate the heat generated by the coil. Yet at the same time, the coil inductance is smaller and the desired current is reached faster, which, along with smaller eddy current losses, results in less heat being generated. With large portions of the reluctance path being nonmagnetic, the level of magnetization in the magnet may reach very low levels, 0.3 T for instance with 2 poles, see Table II. This is a source of concern for high temperature applications. Finally, there is no latching force in the absence of iron, see Table II.

Intermediary solutions should therefore be considered, where the coil is mounted on a thin steel mandrel which carries some flux, provides a latching force and allows better heat dissipation while avoiding large increases of the moving mass and inductance. An optimization process which would balance these contradictory requirements is application specific and therefore beyond the scope of this work. The steel armature, with a desirable latching force and satisfactory heat dissipation, is retained for the remainder of this study.

C. Magnet Pole Design

It is possible to use interpoles between the magnets, either made of steel (Fig. 4) or nonmagnetic (Fig. 5). The results are presented in Table III for three values of interpole-to-pole-pitch ratios. A 0% ratio corresponds to the case with magnets adjacent to one another, the case shown in Fig. 2. Figs. 4 and 5 correspond to 29% ratios.

The acceleration on the coils is approximately the same in all cases, because of the coil concentration (62% of the armature length, (12)). An important difference between these designs, however, is the difference in inductance. With steel interpoles, the inductance is almost twice as much as without steel interpoles. Higher inductances slow down the current rise, thus increasing the copper losses and reducing the initial acceleration. The preference goes in the end to the design with nonmagnetic interpoles because it features a lower inductance and, also, the smallest amount of magnet material.

The magnet could possibly be located behind a flux-concentrating iron pole, in order to focus the flux on the coils. An example is shown in Fig. 6, and many variations of this concept are possible, including buried ring shaped magnets with axial magnetization. This advantage of focusing the flux on the coils, though, is offset by pole-to-pole flux leakage and no configuration with a recessed magnet was found to provide higher force levels. These designs, however, have other features that should be mentioned. A disadvantage, an increased inductance, and several advantages: The volume of ring-shaped magnets is smaller and they are easier to magnetize. Also, the structural integrity of the magnet assembly is improved, and the steel protects the magnets from demagnetization.

D. Preferred Configuration

The illustrations, so far, showed stationary magnets and moving coils. With moving magnets instead, the generated forces are the same but the moving mass is different. In the case illustrated in Fig. 5, the magnet mass is 680 g whereas the mass of the coil assembly is 394 g. Fig. 5 shows also a 470 g iron core behind the magnets, however, this added mass may be avoided as it is possible to design a moving-magnet machine with no iron in the moving armature [7], [11]. Also, placing the coils on the outside and the magnets on the inside will bring the moving mass values

TABLE II
INFLUENCE OF THE ARMATURE DESIGN ON PERFORMANCE

Armature Design	Latching Force (N)	Force with 6000 At (N)	λ ($m/s^2/At$)	λ_c ($m/s^2/At$)	Saturation Level, Maximum (T)	Magnet Magnetization, Minimum (T)
Non-Magnetic, 2 Poles	7	151	0.185	0.185	0.8	0.30
Non-Magnetic, 4 Poles	3	234	0.292	0.292	0.9	0.55
Magnetic, 4 Poles	-394	368	0.322	0.206	2.1	0.70

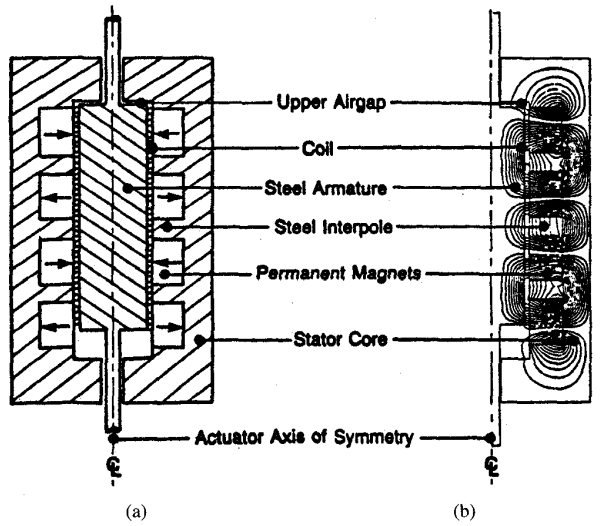

Fig. 4. Configuration with magnetic interpoles. (a) Device layout. (b) Flux plot, no current.

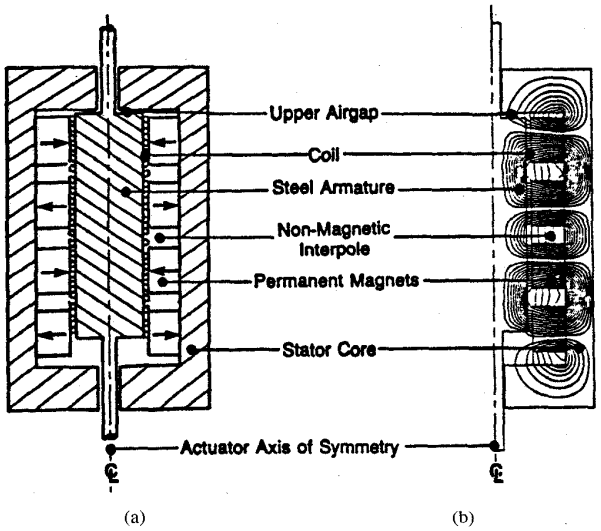

Fig. 5. Configuration with nonmagnetic interpoles. (a) Device layout. (b) Flux plot, no current.

closer together. In the end, however, it appears that moving-magnets assemblies will always be at least as heavy as moving-coil assemblies. In the remainder of the paper, the most favorable situation is assumed, namely, the configuration with nonmagnetic interpoles, with its higher performance, combined with the lower armature mass of a moving coil configuration.

IV. PERFORMANCE EXPECTATION AND COMPARISON WITH 2-SPRING ACTUATORS

It is a characteristic of permanent magnet linear motors that high forces, thus fast travel time, can be obtained with large currents. With modern magnets, the machines can be designed to handle these large currents without demagnetization. Heat dissipation, then, becomes the limit and the fast travel cannot be repeated at a very high rate. Assuming a coefficient $\alpha = 0.7$ (see (A2)), a voltage of 24 V and 100 turns, for instance, the maximum conduction time t_1 is 0.68 ms for 50 operations per second. Per (A6), this yields a travel time of 7.8 ms. More generally, a curve can be drawn to show the minimum travel time as a function of the number of strokes per second, see Fig. 7. The shortest travel time, ca. 1 ms, depends on demagnetization limits not considered here. Also shown on the figure is the number of strokes per second, 90 in this case, at which the machine operates continuously. This is the highest number of strokes possible per second.

For a fast travel over a stoke of 5 to 20 mm, linear motors compete with specially designed solenoids [1], [14]. In particular, 2-spring actuators [1], shown conceptually in Fig. 8, are well suited for this purpose. In 2-spring actuators, when the plunger is at one end of its travel, as shown in Fig. 8, one of the springs (spring A in the figure) is compressed while the other spring (spring B) is released. The compressed spring is held in that state by the permanent magnet. When motion is desired, the coils are excited in such a way as to reduce the level of the magnetic force below that of the spring force, and the spring then drives the plunger to the other end of the stroke. Their performance is compared in Fig. 7 with that of linear permanent magnet motors, on the basis of devices designed for the same stroke (10 mm), within the same volume and for the same level of heat dissipation. The data for the 2-spring actuator was calculated from the experimental data shown in Fig. 8 of [1]. A key characteristic of these devices is that the energy needed for motion is stored, to some extent, in the springs. Therefore, they consume relatively little power and are capable of a high rate of operation. However, their

TABLE III
INFLUENCE OF POLE DESIGN ON PERFORMANCE

Pole Design	Interpole-to-pole Ratio	Latching Force (N)	Force with 6000 At (N)	λ ($m/s^2/At$)	λ_c ($m/s^2/At$)	Inductance (mH)
No Interpole	0%	-394	368	0.322	0.206	0.175
Non-Magnetic InterPole	29%	65	532	0.198	0.193	0.183
Steel Interpole	15%	88	534	0.189	0.184	0.287
	29%	77	524	0.189	0.193	0.323

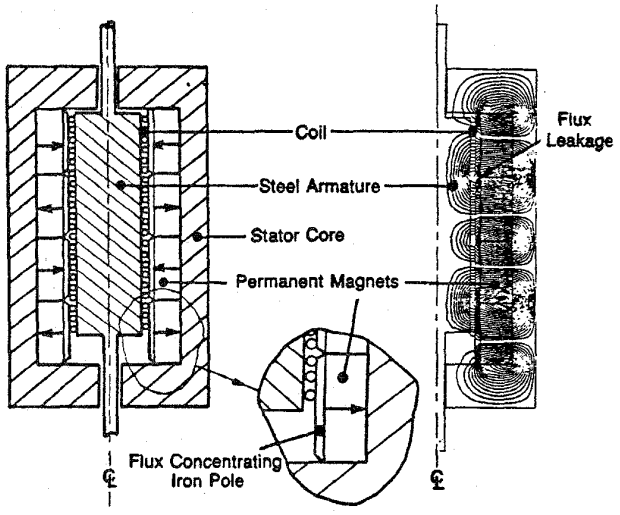

Fig. 6. Recessed-magnet configuration. (a) Device layout. (b) Flux plot, no current.

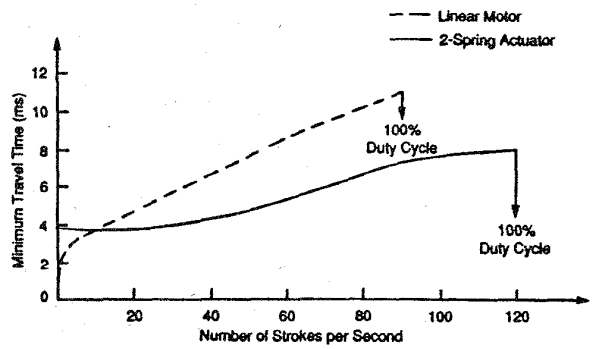

Fig. 7. Limit of operation.

speed of operation is limited by the spring-mass oscillatory frequency, and, as shown in [1], there is a minimum travel time for a given design, 3.9 ms in this case. The linear motor is capable of faster operation on a sporadic basis, but the 2-spring actuator is superior when more frequent operation is desired. The cross-over point in the case of Fig. 7 is at approximately

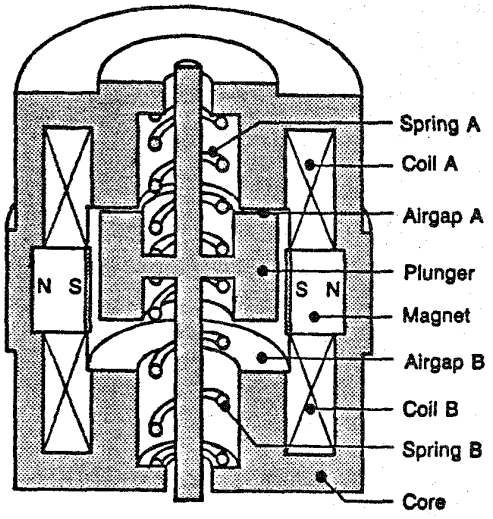

Fig. 8. 2–spring actuator.

12 strokes per second. The 2-spring actuator is capable of ca. 120 strokes per second, 33% more than the linear motor.

In comparing the two devices, other factors must also be taken into account. It was explained in [1] that 2-spring actuators are poor in terms of energy conversion from electrical to mechanical. If a significant amount of mechanical work is necessary, the linear motor will be superior to the 2-spring actuator, though, again, it will be limited in frequency of operation. As far as manufacturing complexity and cost, the moving elements in the 2-spring actuator are the springs and a steel plunger, and no linear motor, whether with moving magnets or coils, can match this simplicity. Overall material cost is comparable. The power electronics drives are of comparable complexity, provided the linear motors use concentrated windings, and thus do not require complex commutation patterns. Finally, the linear motor exhibits a much simpler position controllability. This characteristic is used extensively in positioning applications, and may be useful when both fast motion and controllability are desired.

It is difficult to extend these conclusions for displacements longer than 20 mm, but it is anticipated that the 2-spring concept is limited for longer strokes while linear motors,

by contrast, are capable of any displacement. However with longer strokes, it is not possible to use concentrated windings, and brushes or electronic commutation with a position sensor must be used, adding complexity and cost.

V. Conclusion

This paper presents an evaluation of the possible use of linear motor concepts and new magnet materials for fast actuation over strokes on the order of 5 to 20 mm. Several configurations were studied with the help of a suitable closed-form solution. The designs included concentrated windings to reduce commutation needs and cost. It was also shown that armature lengthening can provide faster travel up to a point beyond which the added mass cancels out the higher forces. Permanent-magnet linear motors can provide very fast motion but are limited by heat-dissipation considerations to relatively low frequencies of operation. If more frequent operation is desired, 2-spring actuators are superior.

Appendix
General Time-Versus-Lift Solution

A. Current Waveform

As explained in Section II, the back-emf can be neglected. The current waveform can therefore by approximated by two linear functions, see Fig. 9,

$$\begin{aligned} &\text{Voltage on } (t < t_1): \quad i = \frac{V}{L}t \\ &\text{Voltage off } (t_1 \le t \le t_2): \quad i = I_p - \frac{R}{L}I_p(t - t_1) \end{aligned} \tag{A1}$$

where t_1 is the time at which the peak current I_p is reached. After $t = t_2$, the current is zero.

For convenience, the coefficient α is introduced as the ratio of the slopes after and before time t_1

$$\alpha = \frac{RI_p}{V}. \tag{A2}$$

The rms current is then

$$I_{\text{rms}} = \frac{V'}{NL'}t_1\left(\frac{f}{3}t_1\frac{1+\alpha}{\alpha}\right)^{(1/2)} \tag{A3}$$

where f is the number of armature trips per second.

B. Maximum Conduction Time

With a maximum current density of 12.4 A/mm^2, typical of well cooled, small machines, and assuming that the coils consist of a 1.5-mm layer spread over a 79-mm long armature, the maximum rms Ampere-turns, $(NI_{\text{rms}})_{\max}$, are 1470 At. More generally, a maximum current-conduction time $(t_1)_{\max}$ can be defined by solving (A3), with the maximum allowable Ampere-turns as a parameter

$$(t_1)_{\max} = \left[\frac{(NI_{\text{rms}})_{\max}}{(V'/L')}\right]^{(2/3)}\left[\frac{f}{3}\frac{1+\alpha}{\alpha}\right]^{-1/3}. \tag{A4}$$

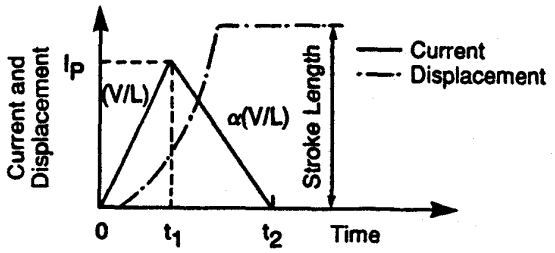

Fig. 9. Current and displacement characteristic.

C. Travel Time

The expressions of the current i in (A1) can be used to integrate the equation of motion (8) to yield the armature position x

$$\begin{aligned} &0 \le t \le t_1: \; x = \lambda\frac{V'}{L'}\frac{t^3}{6} \\ &t_1 \le t \le t_2: \; x = \frac{\lambda V'}{6L'}[t^3 - (1+\alpha)(t-t_1)^2] \\ &t \ge t_2: \qquad x = \lambda\frac{V'}{L'}\frac{t_1^2}{2}\frac{1+\alpha}{\alpha}\left[t - t_1\frac{1+2a}{3a}\right]. \end{aligned} \tag{A5}$$

The travel time t_m is obtained by solving either one of the three expressions in (A5), depending on the expected value of t_m. For instance, if $t_m \ge t_2$

$$t_m = \frac{\alpha}{1+\alpha}\frac{2X_1L'}{\lambda V' t_1^2} + \frac{1+2\alpha}{3\alpha}t_1. \tag{A6}$$

The fastest travel is obtained when $t_1 = (t_1)_{\max}$, where $(t_1)_{\max}$ is a function of the maximum permissible Ampere-turns, see (A4). In all cases, the travel time is minimized when the design ratio (L'/λ) is minimized.

D. Back-EMF

The back-emf e can be calculated as is done in dc-machine theory, which yields

$$e = N\frac{\partial\phi}{\partial x}\dot{x} = \frac{pN}{X_a}\phi_p\dot{x} \tag{A7}$$

where ϕ_p is the flux per pole. The velocity, $\dot{x}$, is calculated by differentiating (A5).

Calculating the back-emf at the end of motion provides a means for estimating the error made by neglecting it. Alternatively, a more accurate value of the travel time can be obtained by first assuming that the back-emf is negligible, then reducing the source voltage V by values of back-emf e_i obtained at various instants t_i, and iterating. Clearly, if the back-emf is expected to be large, this approach cannot be used. It is suited only to machines with a relatively short displacement where the velocity does not reach and stay at significant levels.

References

[1] B. Lequesne, "Fast-acting, long stroke solenoids with two springs," *IEEE Trans. Ind. Applicat.*, vol. 26, no. 5, Sept./Oct. 1990.
[2] K. S. Ananthanarayanan, "Third-order theory and bang-bang control of voice coil actuators," *IEEE Trans. Magn.*, vol. 18, no. 3, pp. 888–892, May 1982.

[3] M. Sri-Jayantha, "Feedback control of impact dynamics of a moving coil actuator," *IEEE Trans. Ind. Electron.*, vol. IE-34, no. 2, pp. 227–284, May 1987.
[4] S. Hasegawa, K. Takaishi, and Y. Mizoshita, "Digital servo control for head-positioning of disk drives," *Fujitusu Sci. Tech. J.*, vol. 26, no. 4, pp. 378–390, Feb. 1991.
[5] S. W. Leung, T. W. S. Chow, and Y. S. Zhu, "An application of linear motor to loudspeaker system," in *IEE Conf. Pub.*, vol. 341, Sept. 1991, pp. 106–109.
[6] Z. Kurtzman, K. O. Stuart, and B. W. Bartosh, "Electromagnetic strut assembly," U.S. Patent 4 892 328, Jan 9, 1990.
[7] K. O. Stuart, "Electromagnetic actuator," U.S. Patent 4 912 343, Mar. 27, 1990.
[8] Anon., "Aura shows magnetic actuator to Detroit crowd," *WARD's Engine Update*, p. 3, May 15, 1990.
[9] L. Honds and K. H. Meyer, "A linear DC motor with permanent magnets," *Philips Tech. Rev.*, Vol. 40, Nos. 11/12, pp. 329–337, 1982.
[10] A. C. Smith and L. C. Appel, "Determing the maximum thrust of a permanent-magnet linear actuator," in *IEE EMDA Conf. Pub.*, vol. 292, Nov. 1987, pp. 344–347.
[11] A. C. Smith, "Magnetic forces on a misaligned rotor of a PM linear actuator," in *Proc. 1990 Int. Conf. Elec. Mach.*, pp. 1076–1081.
[12] A. Basak and G. H. Shirkoohi, "Computation of magnetic field in DC brushless linear motors built with NdFeB magnets," *IEEE Trans. Magn.*, vol. 26, no. 2, pp. 948–951, Mar. 1990.
[13] S. Pelissier, R. Saldanha, J.-P. Yonnet, and J.-L. Coulomb, "Optimization of a linear permanent magnet actuator," *J. Magnetism, Magn. Mater.*, vol. 101, pp. 335–337, 1991.
[14] B. Lequesne, "Fast-acting, long-stroke bistable solenoids with moving permanent magnets," *IEEE Trans. Ind. Appl.*, vol. 26, no. 3, pp. 401–407, May/June 1990.
[15] D. Matt, R. Goyet, J. Lucidarme, and C. Rioux, "Longitudinal-field multi-airgap linear reluctance actuator," *Elect. Mach. Pow. Sys.*, vol. 13, pp. 299–313, 1987.
[16] M. Karita, Y. Sato, H. Yamada, Y. Yamamoto, and Y. Mitamura, "Mock circulatory test of artificial heart using linear pulse motor drive," in *Proc. 1990 Int. Conf. Elec. Mach.*, pp. 1071–1075.
[17] D. A. Torrey and D. M. Orlicki, "A comparison betweeen a permanent magnet and a variable-reluctance distributed torque source," in *Proc. 1990 Int. Conf. Elec. Mach.*, pp. 862–867.
[18] T. W. Nehl, A. M. Pawlak, and N. Mikhaeil-Boules, "ANTIC85: A general purpose finite element package for computer aided design and analysis of electromagnetic devices," *IEEE Trans. Magn.*, vol. 24, no. 1, Jan. 1988.
[19] B. Lequesne, "Finite element analysis of a constant force solenoid for fluid flow control," *IEEE Trans. Ind. Applicat.*, vol. 24, no. 4, July/Aug. 1988.

Bruno Lequesne (M'85-SM'89) received the Certified Engineer degree from the Ecole Superieure d'Electricite, France, in 1978, and the Ph.D. degree in electrical engineering from the University of Missouri-Rolla, in 1984.

He is currently a Staff Research Engineer with the General Motors Research and Development Center in Warren, MI, where his research interests are primarily in the area of the design, analysis, and control of electromagnetic devices, in particular linear actuators and sensors. He holds eight U.S. Patents on automotive actuators and magnetic sensors.

Dr. Lequesne received four Best Paper Awards from the IAS-Electric Machines Committee.